

# Design of a Manipulator System for Hemorrhage Detection and Treatment using High Intensity Focused Ultrasound

Pablo Valdivia y Alvarado, Chu-Yin Chang, and Kullervo Hynynen

**Abstract**—This paper outlines the design of a portable manipulator system for use in remote detection and care of hemorrhage using High Intensity Focused Ultrasound (HIFU). We have developed a kinematically redundant manipulator that uses high fidelity force control for safe interaction with human patients. The manipulator is outfitted with a dual imaging and sonication end-effector for hemorrhage detection and treatment. Unlike most available force controlled manipulators, the design presented in this paper has all the actuation embedded inside its body eliminating the need for a base which greatly improves portability. We review the main design features, advantages, and trade-offs of this approach and present experimental data of hemorrhage detection and controlled sonication of biological tissue samples.

## I. INTRODUCTION

Over 75% of civilian trauma deaths occur in the pre-hospital, or early in hospital phase [1]. On the battlefield, approximately 86% of all combat casualties occur within the first 30 minutes of injury [2]. Emergency care surgeons agree that most deaths from trauma injuries (civilian or battlefield) are preventable if patients can be stabilized during the *golden hour* period [3], [4]. Battlefield injuries present special challenges. Historically, nearly 50% of combat deaths are due to hemorrhage [2]. Of those, it is speculated that about half could be saved if timely, appropriate care were available. Increasingly effective body armor is protecting the torso, yielding an environment in recent conflicts where severe bleeding from injuries to the extremities is emerging as the leading cause of loss of life and permanent injury. Treatment of battlefield casualties is hampered by the long evacuation times often found in military operations. This requires battlefield medics to stabilize patients for extended periods and makes battlefield trauma care markedly different from civilian trauma care. These sobering facts indicate the need for a new technique on the battlefield to treat hemorrhage early and save lives. One technology that holds great promise in this area is High Intensity Focused Ultrasound (HIFU). HIFU has been investigated since early last decade [5], [6], [7], [8], and it has proven to be a valuable non-invasive surgical technique. A HIFU transducer can precisely target acoustic energy on a small volume inside

a tissue sample and increase that volumes temperature to the point of ablation. The tissue surrounding the target remains intact and unharmed. This feature is being studied to cure some cancers, cauterize tumors, and facilitate localized drug delivery. HIFU has also been shown to effectively control bleeding from vessels up to 2 *mm* in diameter and the technology is advancing. It is expected that in the near future, HIFU will effectively control hemorrhage from vessels 8 to 10 *mm* in diameter. For this technology to improve combat casualty care, however, it must be available on the battlefield, even if the expertise needed to operate it is not. What is needed is a way to enable medical personnel remote control of HIFU operations, and to integrate these remotely operated HIFU tools with battlefield trauma and transport equipment. The main challenges are identifying the areas on a patient that need to be treated and stopping or controlling the hemorrhage while interacting safely with the patient. Our group is developing a robotic system which will allow medical personnel to perform the required patient inspection and treatment from virtually anywhere in the world. An earlier manipulator design and preliminary experiments were described in [9], [10].

In this paper we present the design of a new manipulator system with high fidelity force control capabilities. The manipulator can safely interact with human patients, use ultrasound imaging for hemorrhage detection, and use HIFU transducers to ablate tissue and help control hemorrhage. Section II summarizes the design features of the different components of the system. Section III presents experimental data of individual system components. A discussion of the system and its performance can be found in section IV. Section V summarizes the main system characteristics and the principal findings of this study, provides concluding remarks, and some ideas for future work.

## II. SYSTEM DESIGN

The robotic system needs to provide the required tools to allow a trained physician means for safely and accurately inspect and treat patients for uncontrolled hemorrhage. The remote aspect of the interventions requires the use of tele-presence tools and the appropriate hardware and software solutions. The principal requirements of the system are to ensure safe interaction with human patients, to provide a large enough workspace for the user to easily reach, visualize, and treat all of the patient body areas, to provide the user with enough visual and force feedback to carry on interventions, to display high detection and treatment accuracy, and to

This work was supported by the U.S. Army Medical Research and Materiel Command under contract W81XWH-05-C-0159

P. Valdivia y Alvarado and C.Y. Chang are with Energid Technologies, Cambridge MA 02138, USA pablov@energid.com, cyc@energid.com

K. Hynynen is with the Department of Radiology at the Brigham and Women's Hospital, Harvard Medical School, Boston, MA 02115, USA, and with the Department of Medical Biophysics at the University of Toronto, Toronto, ON M4N 3M5, Canada khynynen@sri.utoronto.ca

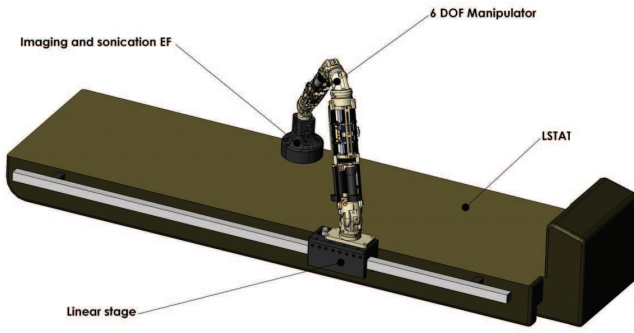


Fig. 1. Manipulator system design mounted on a Life Support for Trauma and Transport (LSTAT) unit.

ensure stability in the presence of disturbances, delays, and communications bandwidth variations.

The robotic system consists of a force controlled manipulator and an end-effector (EF) with ultrasound transducers for visual feedback and treatment. The manipulator can be tele-operated with standard haptic user interfaces or with a duplicate manipulator, as our design enables haptic feedback. Force feedback is essential to allow the user proper regulation of contact forces. The manipulator can be mounted on a linear stage to further extend its workspace. The entire assembly is designed to be easily mounted on operating room tables and also on a Life Support for Trauma and Transport (LSTAT)<sup>1</sup>, a system developed by Integrated Medical Systems (IMS) [11] which is also being evaluated by the Army to enhance future battlefield emergency rooms. Fig. 1 shows the robotic system design and how it can be assembled to an LSTAT unit. Energid's manipulator is being used in studies that target hemorrhage in patient extremities since statistics show the use of body armor, in most cases, limits hemorrhage to those areas and ultrasound treatment of thorax regions is complicated by air pockets (e.g lungs, stomach, etc). For safety, the manipulator feedback can compensate for small motion disturbances and it is assumed the patients will be unconscious and restrained during interventions. The control software can also limit the EF contact forces (20 N is enough to maintain proper pressure for ultrasound visualization and HIFU application). The following sections describe the design and features of each of the system subcomponents.

#### A. Manipulator and linear stage

The robotic system should enable a patient's thorough physical inspection, and due to the complexity of human topology a kinematically redundant manipulator design is

<sup>1</sup>The LSTAT is an advanced platform that allows monitoring and intervention of severely injured patients during transport.

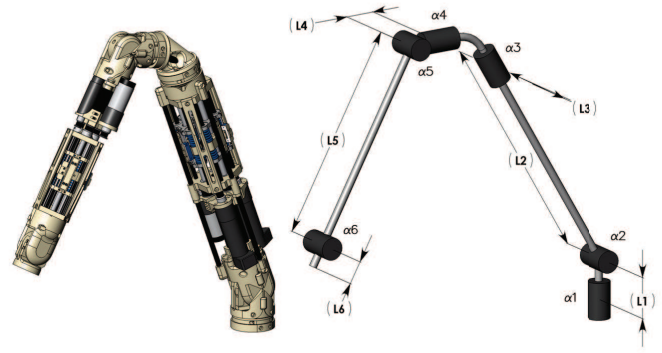


Fig. 2. Manipulator design and corresponding kinematic chain representation. All DOF are revolute joints.

TABLE I  
MANIPULATOR SPECIFICATIONS

Link	Length (m)	Weight (kg)	Joint	Range (rad)	Max. Torque (Nm)
$L_1$	0.07	0.28	$\alpha_1$	$\pm 0.7$	87.9
$L_2$	0.41	2.41	$\alpha_2$	$-0.1 - 0.4$	87.9
$L_3$	0.06	0.26	$\alpha_3$	$\pm 0.7$	27.8
$L_4$	0.05	0.15	$\alpha_4$	$\pm 0.1$	8.7
$L_5$	0.36	1.21	$\alpha_5$	$0 - 1.1$	15.1
$L_6$	0.04	0.12	$\alpha_6$	$\pm 0.8$	8.7

needed. In addition, the system should be capable of controlling all contact forces and torques with a patient to ensure a safe interaction. Both geometry and weight will influence portability and safety around humans. A manipulator with 6 degrees of freedom (DOF) was designed to satisfy the minimum set of controllable forces while keeping weight and complexity at a minimum. Additional DOF, provided by the end-effector and base linear stage, make the system kinematically redundant (a total of 8 DOF). Fig 2 shows an isometric view of the manipulator next to a skeletal representation of its kinematic chain. All DOF in the manipulator are revolute joints. Table I lists values for link geometry, weight, and the range of motion at each joint. All DOF use cable driven transmissions and stiffness based high fidelity force control [12], [13] to achieve high torque to weight ratios. The assembled manipulator weighs 4.43 kg and can easily move payloads of up to 2 kg. Our group has developed a novel way to package 3 stiffness based actuation units on a single link, which enables the inclusion of all required actuation in the arm's body. Three actuators are embedded in the forearm link ( $L_5$ ) and power wrist pitch ( $\alpha_6$ ), elbow pitch ( $\alpha_5$ ), and elbow roll ( $\alpha_4$ ) motions. The actuation arrangement is very similar in the upper arm link ( $L_2$ ) where the actuators that power elbow roll ( $\alpha_3$ ), shoulder pitch ( $\alpha_2$ ), and shoulder roll ( $\alpha_1$ ) motions are housed. Fig. 3

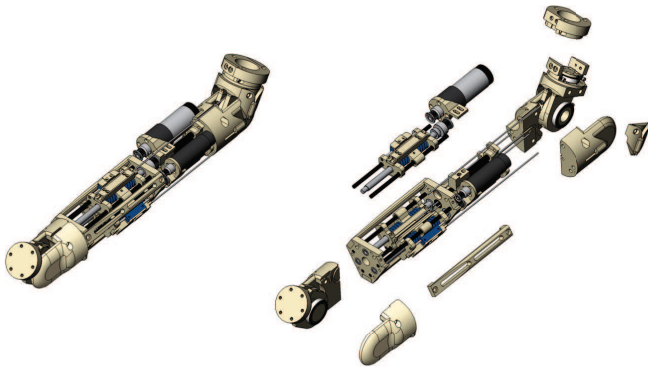


Fig. 3. Isometric and an exploded views of manipulator's forearm. Three cable driven force-controlled actuators are embedded on a link. Each DOF is powered by a single actuator unit.

TABLE II  
LINEAR STAGE SPECIFICATIONS

Stage travel	1.5 m
Payload	9 kg
Weight	5 kg

shows an isometric view along with an exploded view of the manipulator's forearm. The exploded view displays in more detail the actuator arrangement inside the link. All actuator inputs are decoupled. The linear stage features are listed in Table II. The stage has two fixtures that can be used for clamping to an LSTAT unit or a standard bench.

### B. End-effector

A special end-effector was developed to enable detection and treatment of hemorrhage. The main features of the design are shown in Fig. 4, where side and cross-sectional views show how an imaging ultrasound probe is mounted coaxially with an annular HIFU probe. The ultrasound imaging probe is mounted on a small linear stage to enable alignment of the imaging plane with the HIFU focal region. The stage has a resolution of  $10^{-4}$  m. The current HIFU probe design can steer its target focal region along its central axis which adds an additional DOF to the overall system. The HIFU probe is mounted on a tight fitting shell and encapsulated using a heat dissipating epoxy resin that fully waterproofs and protects the transducer electronics against environmental debris. Table III lists the main characteristics of the transducers currently used. Fig. 5 shows details of the end-effector assembly. The assembled end-effector weights 0.8 kg.

### III. SYSTEM PERFORMANCE

The performance of each individual component was tested and preliminary experiments on the overall system are underway. The experimental setup with the assembled system

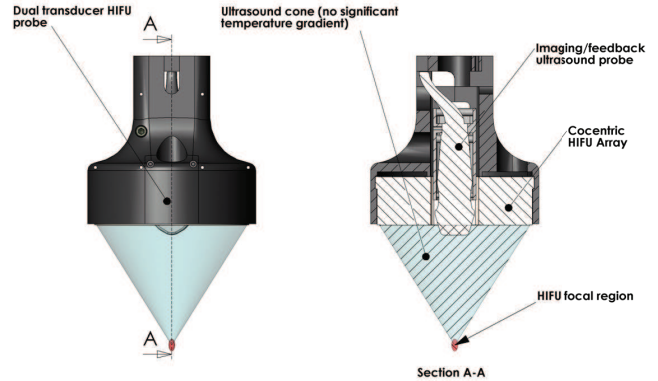


Fig. 4. Dual imaging and sonication end-effector design. An imaging transducer is mounted along the central axis of a annular shaped HIFU probe.

TABLE III  
END-EFFECTOR SPECIFICATIONS

	Imaging Ultrasound	HIFU Transducer
Frequency (MHz)	2 to 5	1 to 1.3
Weight (kg)	0.15	0.10
Range (m)	0 to 0.25	0.06 to 0.18
Power (W)	-	300
Transducer rings	-	20
Expected efficiency (%)	-	50-65
Temperature $\Delta$ (C)	-	70-100

interacting with a biological tissue sample (chicken) is shown in Fig. 6. The manipulator and linear stage are controlled using Energid's ACTIN<sup>TM</sup> control software. The approach, based on English's work [14], uses velocity-control commands derived from position control commands to solve for required joint positions and regulate end-effector motions. The approach, particularly efficient for kinematically redundant chains, can be used to optimize criteria such as balance, collision avoidance, joint-limit avoidance, minimum kinetic energy, and strength optimization. Fig. 7 shows closed loop joint position data of the system using a minimum kinetic energy controller with an without a feedforward (FF) term. Typical steady state maximum position errors are in the order of 0.005 m. Larger transient errors are observed due to hardware control delays. The end-effector performance was also characterized. The HIFU transducer was held in place at the surface of tank filled with degassed and de-ionized water and controlled sonications were performed at different focal targets along the centerline axis ranging from 0.05 m to 0.2 m away from the transducer's face. For each focal target the sound magnitude along the focal region (along the transducer's centerline axis) was measured with a hydrophone. The measured sound magnitudes versus location along the centerline axis are shown in Fig. 8 for all focal targets. Fig.

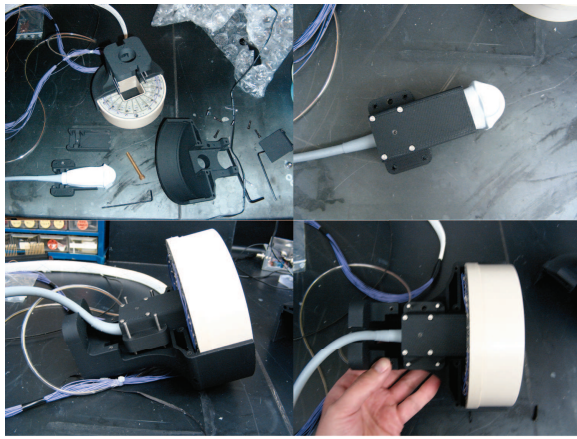


Fig. 5. Details of end-effector assembly. Ultrasound probe is mounted on a 1 DOF stage for alignment. HIFU probe is encapsulated with epoxy for waterproofing and protection against environmental debris.

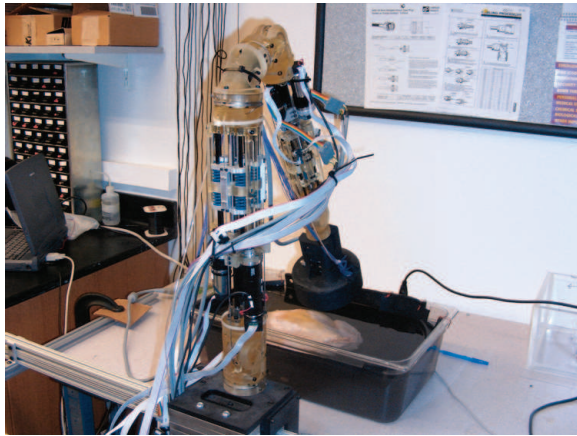


Fig. 6. Manipulator system assembly and experimental setup at the Brigham and Women's Hospital, Boston MA.

8 illustrates the transducer's effective focal range. For our current design, the peak sound magnitude occurs at a focal target  $0.1\text{ m}$  away from the transducer's face and coincides with the observed maximum performance (larger ablation volumes) in biological tissue samples. Areas less than  $0.06\text{ m}$  and more than  $0.18\text{ m}$  away from the transducer face receive too little energy to generate significant ablation. This feature, however, can be tailored by changing the geometry and number of piezo transducers housed inside the probe [15], [16], [17], [18]. For our particular application, this range enables the targeting of most areas of interest inside a patient's body. The sound distributions on the planes along the major and minor axes of the focal region were also measured to visualize the geometry of the focal region. The HIFU transducer was again held in place at the surface of a tank filled with degassed and de-ionized water, and for a given focal target, a hydrophone sensor mounted on an 3 axes stage, scanned the planes along the major axes of the focal region. Fig. 9 shows experimental data for a  $0.1\text{ m}$  focal target with the HIFU transducer power set at 300

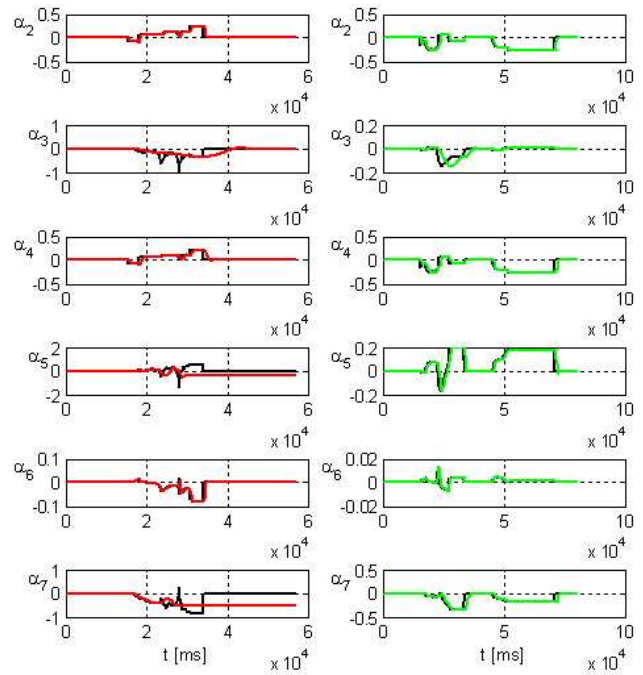


Fig. 7. Closed loop joint position data. Required positions are shown in black, actual positions w/o FF term are shown in red, and actual positions w/ FF term are shown in green. Only inertia terms were used for FF.

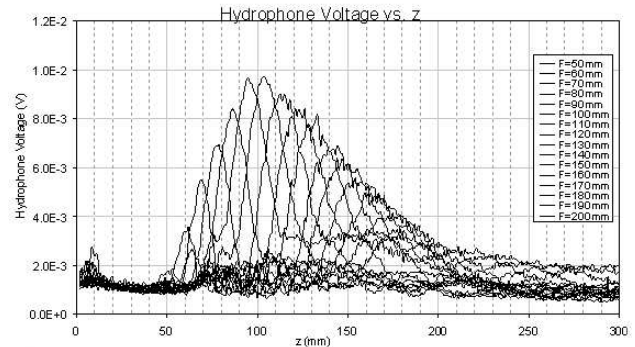


Fig. 8. HIFU transducer sound magnitude across focal region. Data is measured at different target focal regions.

$W$ . The focal region appears as an ellipsoidal volume with a  $0.02\text{ m}$  major diameter and a  $0.01\text{ m}$  minor diameter. This geometry is representative of the largest achievable ablation volume by our current design. Smaller ablations can be achieved by changing the focal target and diminishing transducer's power. Hemorrhage detection using Doppler ultrasound was also tested. Our detection algorithms scan ultrasound images for areas displaying multiple changes in flow direction, characteristic of the turbulence generated by hemorrhage [19], [20]. These areas, due to Doppler's color coding of directional flow, appear as "checker-board" regions [20]. Our algorithm scans the pixels in an image and creates splines around potential hemorrhagic areas. These splines can be edited by a trained user through a computer interface and can then be used to provide position control



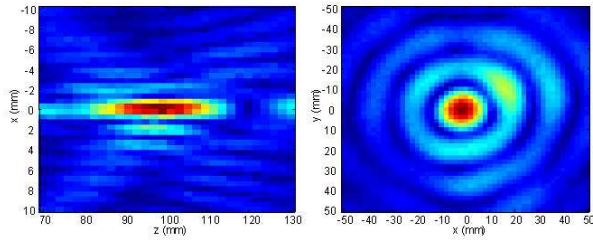


Fig. 9. Pressure distributions along the beam axis (left) and across the focal region (right). The  $x$  and  $y$  axes denote distance across the beam,  $z$  denotes distance away from the transducer.

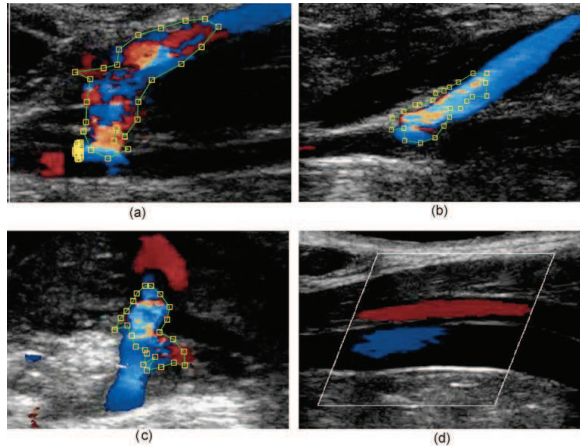


Fig. 10. Hemorrhage detection using Doppler ultrasound imaging. Frames a, b, and c show different cases of potential hemorrhage. Frame d is a control image with normal blood flow.

commands to the manipulator and end-effector assembly. Fig. 10 shows four frames from different movies of in-vivo hemorrhage experiments on animal samples. Frames a), b), and c) display hemorrhage and as a consequence the regions are detected by the algorithm and the hemorrhage areas are selected. Frame d) is a control image that shows normal blood flow, no selection is made by the algorithm. Finally, controlled HIFU sonication was performed on chicken tissue samples. The ultrasound imaging probe allows realtime visualization during HIFU sonication and can be used for position feedback. Fig. 11 shows ultrasound images of a biological tissue sample (chicken) during sonication. The radial lines in the images arise from the interference between the imaging and sonication transducers. Cavitation can be detected after 60 sec, and the focal region can be located in the image as the cavitation bubbles appear bright in the ultrasound image. The samples can be dissected to measure the ablation geometries and confirm the sonication models used for control. A chicken breast sample with HIFU burnt areas is shown in Fig. 12.

#### IV. DISCUSSION

The previous section detailed the performance of the robotic system's individual components. The manipulator and stage assembly workspace allow the user to reach any

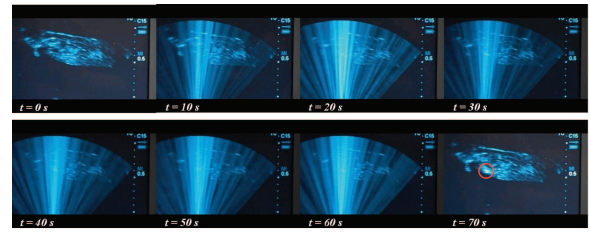


Fig. 11. Ultrasound visualization of HIFU activity. Snapshots at 10 (sec) intervals. Sonicated area appears bright due to cavitation (red circle).

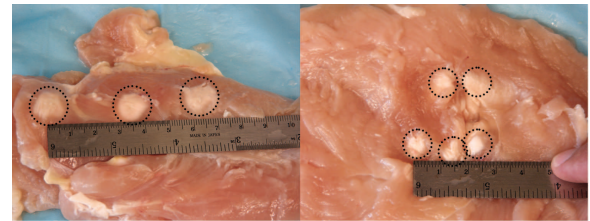


Fig. 12. Biological tissue (chicken breast) sonication samples. Sonicated areas marked by dotted circles. High power sonication cooks areas of up to 0.012 m in diameter.

point on the body of a patient. One particularly useful feature of the manipulator and end-effector assembly is that their combination enables force controlled contact interaction while treatment targets can be controlled by a separate position control loop on the focal region. The only limitation is that, for the present design, the end-effector can only control focal target along its centerline axis. If motions in the orthogonal axes are required to track a target they will be limited by the required by the contact forces and torques. In general, motions due to patient movements and changes in configuration due to contact force control can be treated as disturbances by the focal target position control loop.

The achievable focal range affects treatment applications. Areas of interest on a patient can be anywhere from the surface to deep inside the body, and having the reach flexibility is essential. A useful transducer focal range is normally limited by its geometry, the number of piezo transducers used, and the driving amplifiers. If high power is needed for sonication, as in the case of biological tissue, the focal range is limited. Possible solutions involve developing easily exchangeable, or multi-head end-effectors, having different HIFU probes optimized for different focal ranges. Our current design setup is already tailored for this approach. Another solution is to use ultrasound gel add-ons that can be easily mounted on an end-effector face to artificially place the transducer away from the body surface and be able to reach closer regions with the available focal range. The slight sound attenuation added by the gels will have to be compensated by the position control loop.

Sonication visualization through imaging ultrasound is useful to locate the focal region once cavitation occurs. In the absence of cavitation no position feedback data is available. To address this limitation, look up tables can be generated using models and experimental data of sonication

in different tissues to characterize the appropriate power and control settings needed for a desired focal target. Our current controller already implements this approach, but due to the composite nature of human tissue a larger set of experimental data is needed. Currently, for the largest focal regions, it takes 60 *sec* to achieve cavitation. For hemorrhage control, time is a very important factor and as a result the controller needs to optimize the use of different focal volumes to cover the required target areas in the minimum amount of time. Our group is currently pursuing opportunities to perform experiments with animal models to test the overall system in a more realistic environment.

## V. CONCLUSIONS AND FUTURE WORKS

### A. Conclusions

In this paper we described the robotic system developed for remote hemorrhage detection and treatment using HIFU. The designs and features of a 6 DOF manipulator and a 1 DOF imaging and sonication end-effector were presented. The manipulator and end-effector are light enough to be easily portable yet robust enough to withstand the abuse in harsh environments, which are major requirements in the battlefield. The manipulator's payload is more than adequate for the current end-effector and the force control capabilities are within the safe bounds for human interaction. The manipulator's light weight and reduced inertias also contribute to its inherent safety. The end-effector design is flexible enough to accommodate changes to the HIFU and ultrasound imaging probes. The current linear stage design is tailored mainly to increase the manipulator's workspace and to allow easy assembly to LSTAT units and other surfaces used in emergency rooms. Experimental data that characterizes the performance of individual components and controlled sonication of biological tissue samples was presented. The current robotic system shows great promise for remote hemorrhage detection and treatment and provides a good setup to continue hemorrhage control experiments on animal models. Finally, even though the system features were designed for the battlefield, emergency and civilian first responders can also benefit from them. In these scenarios, the system can help stabilize a patient on its way to the hospital and provide additional expertise via remote link.

### B. Future Works

We expect to continue work in three different areas. First, we plan to proceed with further flow phantoms experiments and pursue opportunities for animal studies. Next, we intend to pursue studies for better non-contact position and temperature feedback to improve sonication targeting. Finally, we plan to continue tele-presence experiments, leveraging a new CODEC technology being developed by our group that can be used to more effectively handle communication delays and communication bandwidth changes.

## VI. ACKNOWLEDGMENTS

The authors gratefully acknowledge the support of the Telemedicine and Advanced Technology Research Center

(TATRC), Ronald Marchessault Jr, and the US Army Medical Research and Materiel Command. The authors would also like to acknowledge Jeffrey Graham, Sai Chun Tan, Charles Seberino, David Askey, James English, John Hu, and Dan Paluska for their contributions to the project, and Dr. Shahram Vaezy and his group at the University of Washington for helpful advice and discussions on using Doppler Ultrasound for hemorrhage detection.

## REFERENCES

- [1] D.D. Trunkey, "Trauma", *Scientific American*, vol. 249, 1983, pp 28-35.
- [2] K. Johnson, F. Pearce, et. al, "Clinical evaluation of the Life Support for Trauma and Transport (LSTAT) platform", *Critical Care Forum*, vol. 6, Issue 5, 2002, pp. 439-446.
- [3] H. Meislin, E.A Criss, et al. "Fatal Trauma: The Modal Distribution of Time to Death Is a Function of Patient Demographics and Regional Resources", *Journal of Trauma-Injury Infection & Critical Care*, vol. 43, No. 3, 1997, pp 433-440.
- [4] L. M. Hussain, A. D. Redmond, "Are pre-hospital deaths from accidental injury preventable?", *BMJ*, vol. 308, 1994, pp 1077-1080.
- [5] S. Vaezy, F. Starr, E. Chi, C. Cornejo, L. Crum, R. Martin, "Intra-Operative Acoustic Hemostasis of Liver: Production of a Homogenate for Effective Treatment", *Ultrasonics*, vol. 43, No. 4, 2005, pp 265-269.
- [6] C. Cornejo, S. Vaezy, G.J. Jurkovich, M. Paun, S.R. Sharar, R.W. Martin, "High Intensity Ultrasound Treatment of Blunt Abdominal Solid Organ Injury: An Animal Model", *J Trauma*, vol. 57, Issue 1, 2004.
- [7] K. Hynynen, "Focused ultrasound surgery guided by MRI", *Science & Medicine*, vol. 3, No. 5, 1996, pp 62-71.
- [8] A. Vanne, and K. Hynynen, "MRI feedback temperature control for focused ultrasound surgery", *Phys. Med.Biol.*, vol. 48, Issue 1, 2003, pp 31-43.
- [9] P. Valdivia y Alvarado, "Tele-Operated Robotic HIFU Manipulator", *Med. Me. Virt. Real. MMVR 16*, Long Beach CA, 2008, <http://www.nextmed.com/pdf/MMVR16-Program-Archive.pdf>
- [10] P. Valdivia y Alvarado, C.Y. Chang, D. Askey, K. Hynynen, and R. Marchessault, "Design of a Teleoperated Robotic Manipulator for Battelfield Trauma Care", *Ame. Telemed. Asso. ATA Meeting* Seattle WA, 2008, <http://www.atmeda.org/conf/2008/presentations.htm>
- [11] Integrated Medical Systems, Life Support for Trauma and Transport, <http://www.lstat.com/>
- [12] G. Pratt and M. Williamson, "Series Elastic Actuators". *Proceedings of the IEEE International Conference on Intelligent Robots and Systems*, vol. 1, 1995, pp 399-406.
- [13] G. Pratt, M. Williamson, P. Dilworth, J. Pratt, K. Ulland, and A. Wright, "Stiffness Isnt Everything". *Proceedings of ISER*, 1995.
- [14] J.D. English and A.A. Maciejewski, "On the Implementation of Velocity Control for Kinematically Redundant Manipulators", *IEEE Trans. on Sys., Man, and Cybernetics Part A: Systems and Humans*, vol. 30, No. 3, 2000, pp 233-237.
- [15] D.R. Daum, and K. Hynynen, "A 256-Element Ultrasonic Phased Array System for the Treatment of Large Volumes of Deep Seated Tissue", *IEEE, Trans. On Ultras. Ferr. And Freq. Cont.*, vol. 46, No. 5, 1999.
- [16] D.R. Daum, M.T. Buchanan, T. Fjield, and K. Hynynen, "Design and Evaluation of a Feedback Based Phased Array System for Ultrasound Surgery", *IEEE, Trans. On Ultras. Ferr. And Freq. Cont.*, vol. 45, No. 2, 1998.
- [17] D.R. Daum, and K. Hynynen, "Thermal Dose Optimization Via Temporal Switching in Ultrasound Surgery", *IEEE, Trans. On Ultras. Ferr. And Freq. Cont.*, vol. 45, No. 1, 1998.
- [18] T. Fjield, and K. Hynynen, "The Combined Concentric-Ring and Sector-Vortex Phased Array for MRI Guided Ultrasound Surgery", *IEEE, Trans. On Ultras. Ferr. And Freq. Cont.*, vol. 44, No. 5, 1997.
- [19] R.W. Martin, S. Vaezy, P. Kaczowski, G. Keilman, S. Carter, M. Caps, K. Beach, M. Plett, L. Crum, "Hemostasis of punctured vessels using Doppler-guided high-intensity ultrasound". *Ultrasound Med Biol*, vol. 25, No. 6, 1999, pp 985-990.
- [20] W. Luo, V. Zderic, F. Mann, S. Vaezy, "Color and Pulsed Doppler Sonography for Arterial Bleeding Detection", *J Ultrasound Med*, vol. 26, No. 8, 2007, pp 1019-1029.